J. Fluid Mech. (2016), *vol.* 786, R3, doi:10.1017/jfm.2015.678

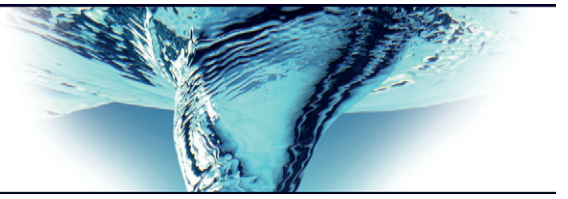

JFM RAPIDS
journals.cambridge.org/rapids

Preferred interparticle spacings in trains of particles in inertial microchannel flows

Soroush Kahkeshani[1], **Hamed Haddadi**[1] **and Dino Di Carlo**[1,†]

[1]Department of Bioengineering, California NanoSystems Institute, University of California, Los Angeles, CA 90095, USA

(Received 11 August 2015; revised 7 October 2015; accepted 10 November 2015; first published online 25 November 2015)

Suspended particles migrate towards inertial focusing positions close to walls and align into trains in finite inertia conduit flow. The relative contribution of inertial and viscous forces at the particle length scale, defined by the particle Reynolds number (Re_p), is a key parameter, where $Re_p = \langle\dot{\gamma}\rangle D^2/\nu$ depends on the mean shear rate $\langle\dot{\gamma}\rangle$, particle diameter D and fluid kinematic viscosity ν. Controlling the location of inertial focusing positions and the interparticle distance is critical in applications such as flow cytometry, imaging and cell entrapment in droplets. By using experimental observations in rectangular microchannels and lattice Boltzmann numerical simulations of dilute suspension flow, the spacing between particles aligned in trains is measured. From the modes of the probability density function of interparticle spacing, preferred spacings at $5D$ and $2.5D$ are observed. At lower Re_p, the preferred spacing forms around $5D$, and with increasing Re_p the spacing at $2.5D$ becomes more pronounced. With increasing concentration of the suspension the spacing is influenced by particle crowding effects until stable trains are no longer observed.

Key words: microfluidics, micro-/nano-fluid dynamics, suspensions

1. Introduction

Migration of particles towards inertial focusing positions and formation of particle trains are prominent examples of inertial effects in flow of dilute suspensions in conduits (Segre & Silberberg 1961; Matas *et al.* 2004). Using a characteristic velocity U, length scale L and fluid kinematic viscosity ν, flow inertia is characterized by Reynolds number defined as $Re = UL/\nu$. In confined geometries, such as microchannels, the inertial flow of dilute suspensions has been utilized to self-assemble particles into trains at inertial focusing positions (Di Carlo *et al.* 2007, 2009; Hur, Tse & Di Carlo 2010; Lee *et al.* 2010). Although the number of trains and the location of focusing positions can be engineered by changing channel dimensions

† Email address for correspondence: dicarlo@seas.ucla.edu

and flow inertia (Chun & Ladd 2006; Amini, Lee & Di Carlo 2014), controlling the interparticle spacing necessitates understanding hydrodynamic interaction between particles. Controlling the distance between particles is crucial for applications such as high-speed imaging, flow cytometry and entrapment of live cells in droplets for tissue printing applications, where knowing the arrival time of particles aids in adjusting the imaging or cell entrapment sequence (Edd *et al.* 2008).

The inertial ordering of particles in trains and interparticle spacings have been experimentally observed in tubular conduits and rectangular microchannels (Matas *et al.* 2004; Hur *et al.* 2010). While the underlying mechanism for inertial migration of particles towards focusing positions can be explained by analytical solution of the lateral force on isolated particles (Ho & Leal 1976; Asmolov 1999; Hood, Lee & Roper 2015), quantitative and predictive models for the spacing between particles self-assembled in trains are more difficult to ascertain due to the complexity of hydrodynamic interactions between multiple moving particles at finite Re (Martel & Toner 2014). By studying inertial flow of a dilute suspension in tubes of $O(10\ \text{mm})$ diameter, the underlying mechanism for train formation was attributed to the presence of reversing streamline regions, where fluid parcels approach the particle surface and reverse their paths (Matas *et al.* 2004). Numerical studies of suspensions of hard spheres at dilute to intermediate concentrations under finite inertia shear flow show that the reversing motion also exists in relative trajectories of particles with respect to one another (Haddadi & Morris 2014, 2015). By increasing Re, the size of the reversing flow region increases, which leads to a shorter distance between particles and a monotonic reduction of the average interparticle spacing in trains (Matas *et al.* 2004). Through experimental study of the reversing streamlines in microchannels, it has been demonstrated that, due to an interplay between viscous disturbance flow, which deviates the particles from inertial focusing points, and inertial lift force, which tends to restore particle location, the average spacing between particles changes until it reaches an equilibrium value in the channel downstream (Lee *et al.* 2010). Although explained in a phenomenological manner, there remains no general predictive model for interparticle spacing. The lateral and axial ordering of particles in microchannels has been studied by changing the concentration of the suspension and the dimensions of the channel cross-section. Increasing the concentration of the suspension leads to formation of multiple trains for certain channel dimensions. A preferred interparticle spacing also forms around $2.2D$ (Humphry *et al.* 2010).

In the present work, experiments and numerical simulations have been employed to study the effect of inertia and concentration on the spacing between particles dynamically self-assembled into trains in microchannels. The axial distance between two consecutive particles, denoted as d_x, depends on the conduit Reynolds number Re_c, which is defined using the hydraulic diameter as the characteristic length scale. Inertia can also be defined at the particle length scale by Re_p, determined by the shear rate and diameter of the particle. For a pressure-driven flow in a channel with rectangular cross-section (channel schematic displayed in figure 1), a parabolic velocity profile along with the difference between channel dimensions in Y and Z directions leads to a varying shear rate on the particle. For a channel with aspect ratio of 0.58, which is defined as $\lambda = l_y/l_z$, particles are expected to equilibrate near the longer walls in the Y direction (Amini *et al.* 2014). Therefore, Re_p can be defined using the mean shear rate, particle diameter D and the channel length in the Y direction (l_y) as $Re_p = (D/l_y)^2 Re_y$, where $Re_y = \langle u \rangle l_y/\nu$. Matas *et al.* (2004) examined the spacing between particles within trains in $O(10\ \text{mm})$ tube flow and reported a monotonic reduction of the average interparticle spacing. Here, the discussion is focused on the most probable

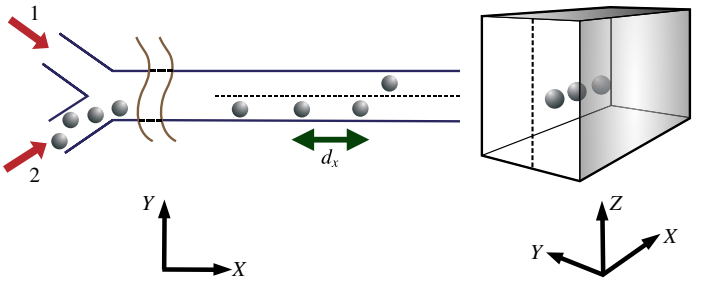

FIGURE 1. Schematic of the channel with two inlets utilized for self-assembly of particles into one train. A particle suspension is pumped from one inlet and fluid without particles is infused from the opposite inlet. Dimensions of the channel in the X (flow), Y (lateral) and Z (transverse) directions are 3 cm, 35 μm and 60 μm respectively, which leads to the formation of two inertial focusing positions near the walls in the Y direction.

spacing between consecutive particles in trains inside a rectangular microchannel, which is important for microchannel imaging and cell sorting applications. In order to measure the location of the most probable spacing, the probability density function of the interparticle distance has been computed for particles self-assembled into trains, and the modes, which distinctly form in curves of the probability density function, are chosen as a metric of the preferred spacing. The effect of Re_p on the axial spacing between consecutive particles (d_x) has been studied for suspensions of concentration $\phi \sim O(0.001)$. It will be shown that the preferred spacing between particles switches from $5D$ for low Re_p to $2.5D$ at higher Re_p, without the presence of intermediate values. The results also demonstrate that increasing the concentration of suspensions to $O(0.01)$ results in the reduction of the distance between particles in trains, and the preferred spacings measured for $\phi \sim O(0.001)$ suspensions will no longer form. Further increase of ϕ leads to unsteadiness in the spacing and prevents self-assembly of particles into ordered trains.

2. Experimental procedure

The experimental observations have been made in a dual-inlet polydimethylsiloxane (PDMS) microchannel bonded to a glass slide produced according to standard soft lithography protocols (Duffy *et al.* 1998). The dual-inlet channel is utilized in order to self-assemble particles predominantly into one train in order to limit hydrodynamic interactions between particles to a single train. Dimensions of the channel in the axial (X or flow direction), lateral (Y) and transverse (Z) directions are 3 cm, 35 μm and 60 μm respectively. A dilute suspension of polystyrene spherical particles with diameter 12 μm ($\rho_p = 1.05$ g cm^{-3}) dispersed in a suspending fluid composed of deionized water, 0.002 weight per volume (w/v) triton X-100 and 0.1 v/v glycerol is pumped into the channel with a controlled flow rate utilizing a syringe pump from one inlet, accompanied by pumping fluid without particles at an equal flow rate from the second inlet. The volume fraction of particles in the suspension is $\phi = 0.004$. More concentrated suspensions of $\phi = 0.011$–0.025 are used to study disruption of trains. The flow rate ranges from 85.5 to 342 μl min^{-1}, leading to finite inertia at $Re_c = 30$–120 inside the channel. Lowering the flow rate below 85.5 μl min^{-1} does not generate sufficient inertia for a steady-state interparticle spacing. Increasing the flow rate above 342 μl min^{-1} leads to experimental errors such as delamination of

the PDMS from the glass slide, leakage at inlets and alteration of the channel size due to high flow-induced deformation in PDMS microchannels (Dendukuri *et al.* 2007). The channel configuration allows formation of particle trains at two inertial equilibrium points close to the walls in the Y direction for $D = 12$ μm particles such that infusing the suspension from one inlet mainly generates a single train close to one wall. The schematics of the channel are displayed in figure 1. The axial distance between two adjacent particles (d_x) has been computed from recorded snapshots captured using high-speed imaging (Phantom V710). The interparticle spacing in multiple sections along the channel has been measured and the values corresponding to the farthest region from the entrance, spanning the last 500 μm section of the channel, have been reported in order to achieve a steady-state spacing.

3. Computational method

In this section, a brief explanation of the governing equations, computational parameters and the lattice Boltzmann method (LBM) that is used to compute particle trajectories in inertial conduit flow is presented. More details about the fundamentals of the LBM are presented in Ladd (1994*a*,*b*) and Nguyen & Ladd (2002), a review article by Aidun & Clausen (2010) and a complete description of Galilean invariance errors due to the presence of particles in Clausen & Aidun (2009). The non-dimensional forms of the equations governing the fluid phase are

$$\boldsymbol{\nabla} \cdot \boldsymbol{u} = 0, \tag{3.1}$$

$$Re\left(\frac{\partial \boldsymbol{u}}{\partial t} + \boldsymbol{u} \cdot \boldsymbol{\nabla} \boldsymbol{u}\right) = -\boldsymbol{\nabla} p + \nabla^2 \boldsymbol{u}, \tag{3.2}$$

where length has been non-dimensionalized using the hydraulic diameter h_d, velocity by the average fluid velocity at the channel inlet $\bar{U}$ and the pressure by $\rho \bar{U}^2$. The LBM algorithm for suspensions of hard spheres, which has been developed by Ladd (1994*a*,*b*) with further improvement for moving particles by Aidun, Lu & Ding (1998), is based on the Boltzmann equation for the fluid phase coupled with Newtonian dynamics for solid particles. By computing the force $\boldsymbol{F}_i$ and torque $\boldsymbol{T}_i$ exerted by the fluid on a particle of mass m_i and moment of inertia I_i, the translational velocity $\boldsymbol{V}_i$ and rotational velocity $\boldsymbol{\Omega}_i$ of the particle are calculated as

$$m_i \frac{\mathrm{d}\boldsymbol{V}_i}{\mathrm{d}t} = \boldsymbol{F}_i, \tag{3.3}$$

$$I_i \frac{\mathrm{d}\boldsymbol{\Omega}_i}{\mathrm{d}t} = \boldsymbol{T}_i. \tag{3.4}$$

In order to calculate particle trajectories in a confined conduit, a rectangular computational box with $128 \times 36 \times 65$ lattice units in X, Y and Z directions is chosen, where X indicates the direction of the flow. The rectangular box is periodic in the flow direction and is confined by solid walls in the Y and Z directions. The specified dimensions of the computational box are chosen in accordance with the dimensions of the microchannel, which leads to observation of two equilibrium points close to the walls in the Y direction. The resolution of the particles was set at 12.9 lattice units (lu) per diameter. The results of the numerical trajectory analysis were found to be independent of further increase in the resolution by simulating particles with a larger size of $D = 16.5$ lu in a $256 \times 72 \times 130$ lu^3 channel. In addition, the results have been examined to be independent of the periodicity in the flow direction by iterating some sample trajectories for a $256 \times 36 \times 65$ lu^3 box.

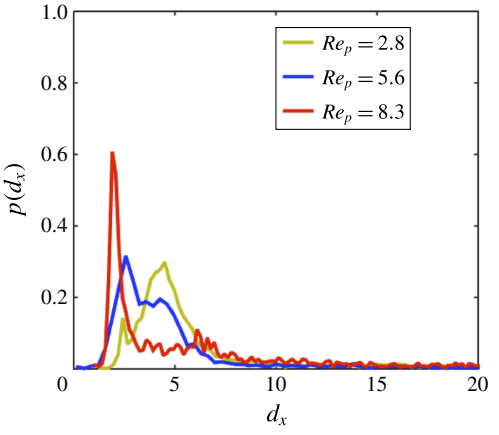

FIGURE 2. The probability density functions (p.d.f.) of axial spacing between particles, d_x, for $Re_p = 2.8$, 5.6 and 8.3 (corresponding to $Re_c = 30$, 60 and 90). The aspect ratio of the channel cross-section is $\lambda = l_y/l_z = 0.58$ and the particle diameter is $D = 12$ μm. With a slight deviation ($<0.4D$), the formation of most probable spacings is observed around $2.5D$ and $5D$, the modes (highest peaks) in the p.d.f.

4. Results and discussion

In figure 2, the probability density functions (p.d.f.) of d_x for $Re_p = 2.8$, 5.6 and 8.3 are presented. The highest peak in the p.d.f. corresponds to the most probable spacing between two consecutive particles at a certain Re_p. Although the adverse effect of particle sedimentation was minimized by matching the density of particles and the fluid, fluctuation in the number of particles observed in each imaging snapshot is inevitable. Considering that the concentration of suspensions used for inertial self-assembly applications is small ($\phi < O(0.01)$), the average length fraction defined as $\langle L_f \rangle = \langle N \rangle D/L$, where $\langle N \rangle$ is the average number of particles per frame monitored throughout the experiment and L is the frame length ($\simeq$500 μm in the present study), can be used as a replacement for volume fraction ϕ (Di Carlo 2009). The average length fraction $\langle L_f \rangle$ is a direct measure for proximity between particles, which affects hydrodynamic interactions. In the experimental measurements discussed here, d_x is compared in trains with identical $\langle L_f \rangle$. This approach assists in differentiating the influence of Re_p on spacing from possible effects of fluctuations in the number of particles in trains. In the probability density functions of figure 2 the value of $\langle L_f \rangle$ is 0.1. It is observed in figure 2 that for $Re_p = 2.8$ the preferred spacing, which corresponds to the peak in the p.d.f. curves, forms around $\simeq 5D$, and for high Re_p of 8.3, the preferred spacing is located around $2.5D$. When varying Re_p, no intermediate preferred spacing is observed and peaks of the p.d.f. are consistently observed around $2.5D$ and $5D$.

Although infusing the suspension from a separate inlet increases the probability of forming one train with axial alignment of particles, i.e. axial ordering, a small number of particles may migrate towards the opposite wall. Sporadic migration of particles towards the opposite wall can start at the channel inlet and during merging. Two consecutive particles that are located on opposite sides of the channel form a lateral ordered pair. The peaks observed in the p.d.f. curves correspond to the spacing between consecutive particles, without distinguishing between axial and

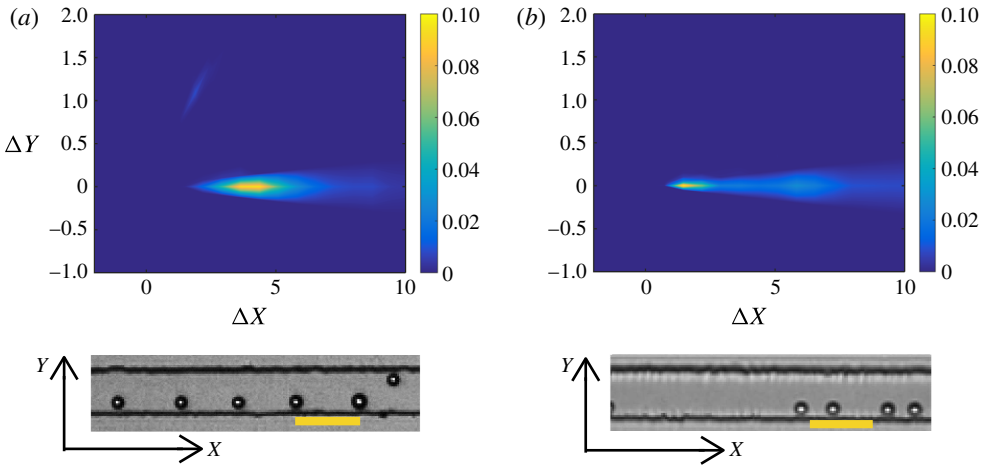

FIGURE 3. The spatial probability distribution of finding the adjacent particle in the vicinity of a reference particle $p(\boldsymbol{r})$ at (*a*) $Re_p = 2.8$ and (*b*) $Re_p = 8.3$. A streak of low probability that is observed at $\Delta X \approx 2.5D$ and $\Delta Y \approx 1.2D$ corresponds to laterally ordered pairs of particles. Snapshots taken from experiments are included to exhibit the self-assembled trains (the scale bar shows a length of 60 μm).

lateral ordered pairs. To make a distinction between axial and lateral orientations, the spatial probability distribution of neighbouring particles is presented in figure 3. The spatial probability distribution, $p(\boldsymbol{r})$, is obtained by constructing a histogram around each particle which is populated by the location of adjacent particles. The histogram is normalized by the total number of samplings. Considering that the pair orientation vector is used to construct the histograms, the distributions span the entire space around the reference particle, including negative X and Y values, although the probability of occupying negative locations is not significant. It is observed in figure 3 that at $Re_p = 2.8$, particle pairs with axial ordering ($\Delta Y = 0$) equilibrate close to $d_x \simeq 5D$. With increasing inertia to $Re_p = 8.3$, the preferred spacing between particles forms around $2.5D$. In the spatial representation of $p(\boldsymbol{r})$ at $Re_p = 2.8$, a secondary zone at $d_x \simeq 2.5D$ is also seen due to the lateral pair configuration ($\Delta Y \neq 0$), which results in the formation of a secondary peak around $2.5D$ in the probability density functions of figure 2. The spacing between particles with lateral ordering has been predominantly observed around $2.5D$ for all Re_p studied.

Humphry *et al.* (2010) measured the axial spacing between particles in single-inlet channels and reported $d_x \simeq 2.2D$, mainly for suspensions flowing at $Re_p \sim O(1)$ in microchannels. Considering that inertial flow of a dilute suspension in a single-inlet channel leads to the formation of particle trains close to both walls, the probability of observing lateral ordering increases. Therefore, an axial spacing of $2.2D$ between particles agrees well with our results.

Experimental observation of interparticle spacing at preferred axial locations of $d_x \simeq 2.5D$ and $5D$ can be further investigated using numerical simulations of particle relative motions. The classes of relative motion of particles in a dilute suspension can be assembled from trajectories of isolated pairs of particles (Haddadi & Morris 2014). Pair trajectories are obtained by calculating the trajectory of one particle with respect to the coordinate frame located at the centre of mass of the second particle. The LBM has been utilized for studying trajectories, and has been proven to be an

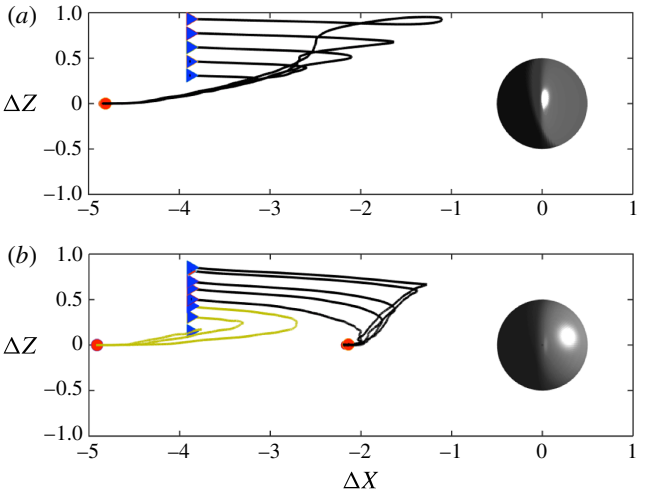

FIGURE 4. Selected pair trajectories calculated numerically at (*a*) $Re_p = 2.8$ and (*b*) $Re_p = 8.3$ projected on the XZ plane. Blue triangles correspond to the starting points of the second particle relative to the reference particle shown at the origin, and red circles correspond to the final steady-state separations.

efficient technique for numerical simulation of inertial suspension flow. The evolution of sample pair trajectories until reaching a steady-state separation at $Re_p = 2.8$ and 8.3 is demonstrated in figure 4. To identify the most probable pair separation at each Re_p, the steady-state separation of pair trajectories with various initial configurations has been examined numerically. A large number of initial configurations, composed of 107 pair orientations for each Re_p, have been simulated to construct a thorough representation of the relative motions. The steady-state pair separations are used to populate a spatial histogram that is constructed around the reference particle. The spatial probability densities of pair equilibrium separations for $Re_p = 2.8$ and 8.3 are shown in figure 5(*a*,*b*) respectively. It is seen that at $Re_p = 2.8$ and for all initial configurations, the most probable spacing for an axially ordered pair is located at $5D$. For pairs with lateral orientation, the preferred spacing forms at $d_x = 2.5D$. At $Re_p = 8.3$, axially ordered spacings at $2.5D$ and $5D$ are more pronounced, where the probability of reaching an equilibrium at $2.5D$ is significantly higher. In addition, pairs with lateral ordering tend to equilibrate at $2.5D$ from the reference particle for all Re_p values.

The match between preferred spacings observed in experiments (figures 2 and 3) and the steady-state separations between pairs in numerical simulations (figure 5) implies that a finite number of attractors contribute to the formation of preferred interparticle spacings in trains. The attractor with highest probability at low Re_p is located at $5D$. With increasing Re_p, rather than a gradual shift in the location of the attractors, the probability of the $5D$ attractor decreases and the $2.5D$ attractor becomes more probable. Using numerical simulations of the disturbance streamlines around a single force-free particle moving in a rectangular channel, the equilibrium distance between two particles has been related to the formation of closed-streamline regions adjacent to the particle (Humphry *et al.* 2010). Considering that the disturbance streamlines around a single particle are affected by the presence of other particles, the fundamental description of the flow leading to formation of attractors remains

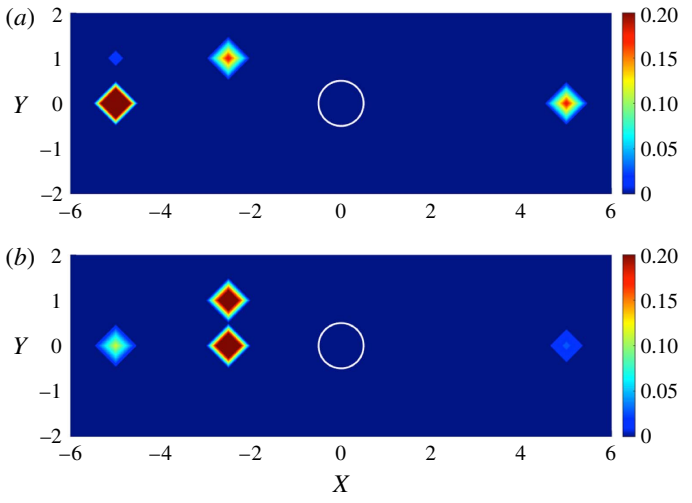

FIGURE 5. Attractors at preferred spacings and their probabilities, calculated by simulating the motion of pairs starting from various initial configurations at (*a*) $Re_p = 2.8$ and (*b*) $Re_p = 8.3$. The boundary of the reference particle is also indicated in the figure. The figure comprises attractors forming in axial and lateral directions. Attractors form at $5D$ and $2.5D$, and the most probable axial attractors are located at $5D$ for $Re_p = 2.8$ and at $2.5D$ for $Re_p = 8.3$. Attractors of lateral orientation are located at $2.5D$ for both Re_p values.

an open question. It should be noted that pair trajectory attractors are not particular to confined inertial flows and have also been observed in the relative motion of particles in Stokes flow of dilute suspensions in two-dimensional microchannels, where linearity of the equations governing Stokes flow allows analytical progress (Uspal & Doyle 2012). It should be emphasized that in the present work, the location of the attractors in the pair trajectory space is obtained from numerical sampling of the pair motion. Although a large number of initial pair configurations have been simulated to calculate the location of attractors, drawing a definite conclusion about the total number and location of pair trajectory attractors is not possible. However, the combination of experimental observations and numerical sampling of the pair space corroborates the existence of preferred spacings between adjacent particles at each Re_p. We also note that there is a deviation (between $0.2D$ and $0.4D$ for the location of the preferred spacings) from the $2.5D$ and $5D$ attractors in experimental measurements. This deviation may be due to unavoidable experimental limitations, including pixel size accuracy in image processing, dispersion in particle size distributions and the presence of multiple particles in a train (more than an isolated pair), which does not exist in simulations of an isolated pair.

The question arises of whether the locations of the attractors depend strongly on the channel and particle size or are more generally observed. The generality has been examined for selected particle sizes and dimensions of the channel cross-section. The locations of the attractors are measured for $Re_p = 2.8$ and 8.3, where the preferred spacing for $D = 12$ μm in $\lambda = 0.58$ channels has been previously explained to be respectively around $5D$ and $2.5D$. Similarly, for $D = 4.8$ and 20 μm particles in $\lambda = 0.58$ channels the location of the attractors remained unchanged. Identically, for $D = 12$ and 20 μm in a $\lambda = 1$ channel ($l_y = l_z = 60$ μm), the attractors at $Re_p = 2.8$ and 8.3 form around $5D$ and $2.5D$.

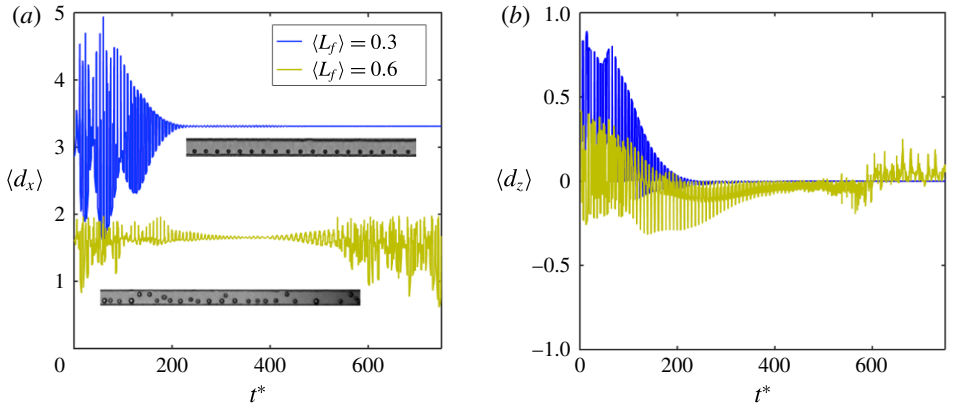

FIGURE 6. Variation of average spacing between particles versus time for larger concentrations of particles: (*a*) average axial separation $\langle d_x \rangle$ at $Re_p = 2.8$ and (*b*) average transverse separation $\langle d_z \rangle$ at $Re_p = 2.8$. Dimensionless time is defined as $t^* = t\langle U \rangle / D$.

For inertial self-assembly of particles in trains, the average length fraction of particles $\langle L_f \rangle$ in trains is an important parameter in addition to Re_p. Attaining a tangible increase in length fraction is achieved by increasing the volume fraction ϕ to $O(0.01)$. It has been shown that increasing ϕ leads to formation of multiple trains in microchannels with large aspect ratios of the channel cross-section (Humphry *et al.* 2010). In order to study the spacing between particles for a more concentrated suspension, experiments have been conducted at $\phi = 0.011$–0.025, which results in $\langle L_f \rangle \simeq 0.3$–$0.6$. (It should be noted that $\langle L_f \rangle = 0.1$ is achieved at $\phi = 0.004$.) The volume fraction of suspensions is still considered to be in a dilute rheological regime; however, increasing ϕ to $O(0.01)$ leads to a pronounced increase of $\langle L_f \rangle$ to 0.6, which can alter the dynamic self-assembly of particles into trains. Numerical simulations have also been conducted and the average distance between pairs of consecutive particles versus time has been monitored. Figure 6(*a*) shows numerical values of $\langle d_x \rangle$ versus dimensionless time $t^* = t\langle U \rangle / D$ ($\langle U \rangle$ is the average inlet velocity) at $Re_p = 2.8$ and includes snapshots taken from experimental measurements. For numerical simulations of larger $\langle L_f \rangle$, the number of particles in the computational box has been increased without changing the box size. The average distances between particles in X and Z directions, denoted as $\langle d_x \rangle$ and $\langle d_z \rangle$ respectively, are computed as the average centre-of-mass separations of particle pairs in each time step. It is observed that with increasing $\langle L_f \rangle$ to 0.3 (three times higher than previous results) the preferred axial spacing decreases to $\simeq 3.2D$ from the previously observed $5D$ for $\langle L_f \rangle \simeq 0.1$. Although at $\langle L_f \rangle \simeq 0.3$ particles are still self-assembled into ordered trains and the final $\langle d_x \rangle$ reaches a steady value, with further increase of $\langle L_f \rangle$ to 0.6 interparticle distance starts to fluctuate, which prevents the formation of a self-assembled train, as can be seen in experimental snapshots. The disruption of trains can be viewed as fluctuations of spacing in either y or z direction computed numerically. Figure 6(*b*) exhibits $\langle d_z \rangle$ for $\langle L_f \rangle = 0.3$ and 0.6, where apparent temporal fluctuations in spacing and disruption of particle ordering are seen at $\langle L_f \rangle = 0.6$.

5. Conclusion

The experimental measurements of the distance between consecutive particles self-assembled in trains, which have been validated by numerical simulations, can

be used as a predictive model for dynamic self-assembly of particles with precise separations from one another. Depending on the Re_p, the most probable spacings in a dilute regime of $\phi = O(0.001)$, corresponding to 'trajectory attractors', are located around $2.5D$ and $5D$. The attractors appear to be generally observed for varying ratios of particle size to channel dimensions and channel aspect ratios, although a more exhaustive investigation of the space would be required to confirm this result. By increasing the concentration of suspensions to $\phi = O(0.01)$, the spacing between particles decreases until it reaches an unsteady state spacing where focusing of the particles into trains is no longer possible. The results could be helpful in practical applications, suggesting the ability to make use of either of the two attractors if flow conditions are controlled precisely.

Acknowledgements

The support from ONR Young Investigator Program is acknowledged. We would like to thank Professor A. Ladd at University of Florida–Gainsville for providing the initial lattice Boltzmann solver.

References

AIDUN, C. K. & CLAUSEN, J. R. 2010 Lattice-Boltzmann method for complex flows. *Annu. Rev. Fluid Mech.* **42**, 439–472.

AIDUN, C. K., LU, Y. & DING, E. 1998 Direct analysis of particulate suspensions with inertia using the discrete Boltzmann equation. *J. Fluid Mech.* **373**, 287–311.

AMINI, H., LEE, W. & DI CARLO, D. 2014 Inertial microfluidic physics. *Lab on a Chip* **14**, 2739–2761.

ASMOLOV, E. S. 1999 The inertial lift on a spherical particle in a plane Poiseuille flow at large channel Reynolds number. *J. Fluid Mech.* **381**, 63–87.

CHUN, B. & LADD, A. J. C. 2006 Inertial migration of neutrally buoyant particles in a square duct: an investigation of multiple equilibrium positions. *Phys. Fluids* **18**, 031704.

CLAUSEN, J. R. & AIDUN, C. K. 2009 Galilean invariance in the lattice-Boltzmann method and its effect on the calculation of rheological properties in suspensions. *Intl J. Multiphase Flow* **35**, 307–311.

DENDUKURI, D., GU, S. S., PREGIBON, D. C., HATTON, T. A. & DOYLE, P. S. 2007 Stop-flow lithography in a microfluidic device. *Lab on a Chip* **7**, 818–828.

DI CARLO, D. 2009 Inertial microfluidics. *Lab on a Chip* **9**, 3038–3046.

DI CARLO, D., EDD, J. F., HUMPHRY, K. J., STONE, H. A. & TONER, M. 2009 Particle segregation and dynamics in confined flows. *Phys. Rev. Lett.* **102**, 094503.

DI CARLO, D., IRIMIA, D., TOMPKINS, R. G. & TONER, M. 2007 Continuous inertial focusing, ordering, and separation of particles in microchannels. *Proc. Natl Acad. Sci. USA* **104**, 18892–18897.

DUFFY, D. C., MCDONALD, C. J., SCHUELLER, O. J. A. & WHITESIDES, G. M. 1998 Rapid prototyping of microfluidic systems in poly(dimethylsiloxane). *Anal. Chem.* **70**, 4974–4984.

EDD, J. F., DI CARLO, D., HUMPHRY, K. J., KOSTER, S., IRIMIA, D., WEITZ, D. A. & TONER, M. 2008 Controlled encapsulation of single-cells into monodisperse picolitre drops. *Lab on a Chip* **8**, 1262–1264.

HADDADI, H. & MORRIS, J. F. 2014 Microstructure and rheology of finite inertia neutrally buoyant suspensions. *J. Fluid Mech.* **749**, 431–459.

HADDADI, H. & MORRIS, J. F. 2015 Topology of pair-sphere trajectories in finite inertia suspension shear flow and its effects on microstructure and rheology. *Phys. Fluids* **27**, 043302.

HO, B. P. & LEAL, L. G. 1976 Migration of rigid spheres in a two-dimensional unidirectional shear flow of a second-order fluid. *J. Fluid Mech.* **76**, 783–799.

HOOD, K., LEE, S. & ROPER, M. 2015 Inertial migration of a rigid sphere in three-dimensional Poiseuille flow. *J. Fluid Mech.* **765**, 452–479.

HUMPHRY, K. J., KULKARNI, P. M., WEITZ, D. A., MORRIS, J. F. & STONE, H. A. 2010 Axial and lateral particle ordering in finite Reynolds number channel flows. *Phys. Fluids* **22**, 081703.

HUR, S. C., TSE, H. T. K. & DI CARLO, D. 2010 Sheathless inertial cell ordering for extreme throughput flow cytometry. *Lab on a Chip* **10**, 274–280.

LADD, A. J. C. 1994*a* Numerical simulations of particulate suspensions via a discretized Boltzmann equation. Part 1. Theoretical foundation. *J. Fluid Mech.* **271**, 285–309.

LADD, A. J. C. 1994*b* Numerical simulations of particulate suspensions via a discretized Boltzmann equation. Part 2. Numerical results. *J. Fluid Mech.* **271**, 311–339.

LEE, W., AMINI, H., STONE, H. A. & DI CARLO, D. 2010 Dynamic self-assembly and control of microfluidic particle crystals. *Proc. Natl Acad. Sci. USA* **107**, 22413–22418.

MARTEL, J. & TONER, M. 2014 Inertial focusing in microfluidics. *Annu. Rev. Biomed. Engng* **16**, 371–396.

MATAS, J. P., GLEZER, V., GUAZZELLI, E. & MORRIS, J. F. 2004 Trains of particles in finite-Reynolds-number pipe flow. *Phys. Fluids* **16**, 4192–4195.

NGUYEN, N. Q. & LADD, A. J. C. 2002 Lubrication corrections for lattice-Boltzmann simulations of particle suspensions. *Phys. Rev.* E **66**, 046708.

SEGRE, G. & SILBERBERG, A. 1961 Radial particle displacements in Poiseuille flow of suspensions. *Nature* **189**, 209–210.

USPAL, W. E. & DOYLE, P. S. 2012 Collective dynamics of small clusters of particles flowing in a quasi-two-dimensional microchannel. *Soft Matt.* **8**, 10676–10686.